Biotransformation of *p*-Coumaric Acid (=(2*E*)-3-(4-Hydroxyphenyl)prop-2-enoic Acid) by *Momordica charantia* Peroxidase

by **Hai-Li Liu**, **Xue-Feng Huang**, **Xiang Wan**, and **Ling-Yi Kong***

Department of Natural Medicinal Chemistry, China Pharmaceutical University; 24 Tong Jia Xiang, Nanjing 210009, P. R. China
(phone: +86-25-85391289; fax: +86-25-85301528; e-mail: lykong@jlonline.com)

LC/MS^3-Guided biotransformation of *p*-coumaric acid (=(2*E*)-3-(4-hydroxyphenyl)prop-2-enoic acid; CA) with H_2O_2/*Momordica charantia* peroxidase at pH 5.0 and 45° in the presence of acetone has resulted in the isolation of three CA trimers, triCA1 (**1**), triCA2 (*trans*-**2**), and triCA3 (*cis*-**2**), and seven CA dimers, diCA1–diCA7, *i.e.*, **3**–**9**, among which seven (triCA1–triCA3 and diCA1–diCA4) are new compounds and three (diCA5–diCA7) are known compounds. The structures were established by 2D-NMR such as HSQC, HMBC, and NOESY measurements. The possible mechanism for the formation of the products is also discussed (*Schemes 1–3*). This is the first time that the biotansformation of *p*-coumaric acid catalyzed by peroxidase *in vitro* was achieved. Compounds triCA3 (*cis*-**2**), diCA1 (**3**), diCA5 (**7**), and diCA7 (**9**) exhibit a stronger antioxidative activity than the parent CA.

1. Introduction. – Previously, we reported the physical and chemical characterization of *Momordica charantia* peroxidase (MCP), a novel plant peroxidase, rich in acidic amino acid, isolated from the fruits of *Momordica charantia* [1]. We found that although MCP shared spectral and kinetic features with other peroxidases, the enzyme had several unique characteristics, including enzyme pH stability (pH 3.8–8.0) and a wider thermostability (20–45°) than that of other peroxidases such as horseradish peroxidase [2]. So, MCP can be expected to oxidize a broader range of substrates, especially cinnamic acid derivatives, when considering the potential applications of MCP for useful biotransformations.

The *p*-coumaric acid (=4-hydroxycinnamic acid=(2*E*)-3-(4-hydroxyphenyl)prop-2-enoic acid; CA), which is also an abundant phenolic natural product, exhibited antioxidant property [3]. In recent years, microbial and plant cell suspension cultural transformation screening studies of CA have been carried out, and a series of products have been obtained including 4-hydroxybenzoic acid, protocatechuic acid [4–6], 4-vinylphenol [7–11], caffeic acid [12][13], 4-ethylphenol [14], and so on. CA Hydroxylases [12][13] and a decarboxylase [9][11][14][15] were involved in the conversion of those metabolites of CA. However, only two CA dimers [16] were reported, and CA trimers have never been obtained. Furthermore, the biotransformation of CA catalyzed by pure peroxidase *in vitro* has never been reported.

To study the biotransformation of CA by the purified MCP *in vitro* and analyze CA trimers and CA dimers, we investigated the oxidative coupling of CA with H_2O_2/MCP at pH 5.0 and 45° in the presence of acetone guided by means of LC/MS^3. Three CA

trimers, triCA1 – triCA3, *i.e.*, **1**, *trans*-**2**, and *cis*-**2**, and seven CA dimers, diCA1 – diCA7, *i.e.*, **3** – **9**, were found (*Fig. 1*), among which seven, *i.e.*, triCA1 (**1**), triCA2 (*trans*-**2**), and triCA3 (*cis*-**2**) and diCA1 (**3**), diCA2 (**4**), diCA3 (**5**), and diCA4 (**6**), are new

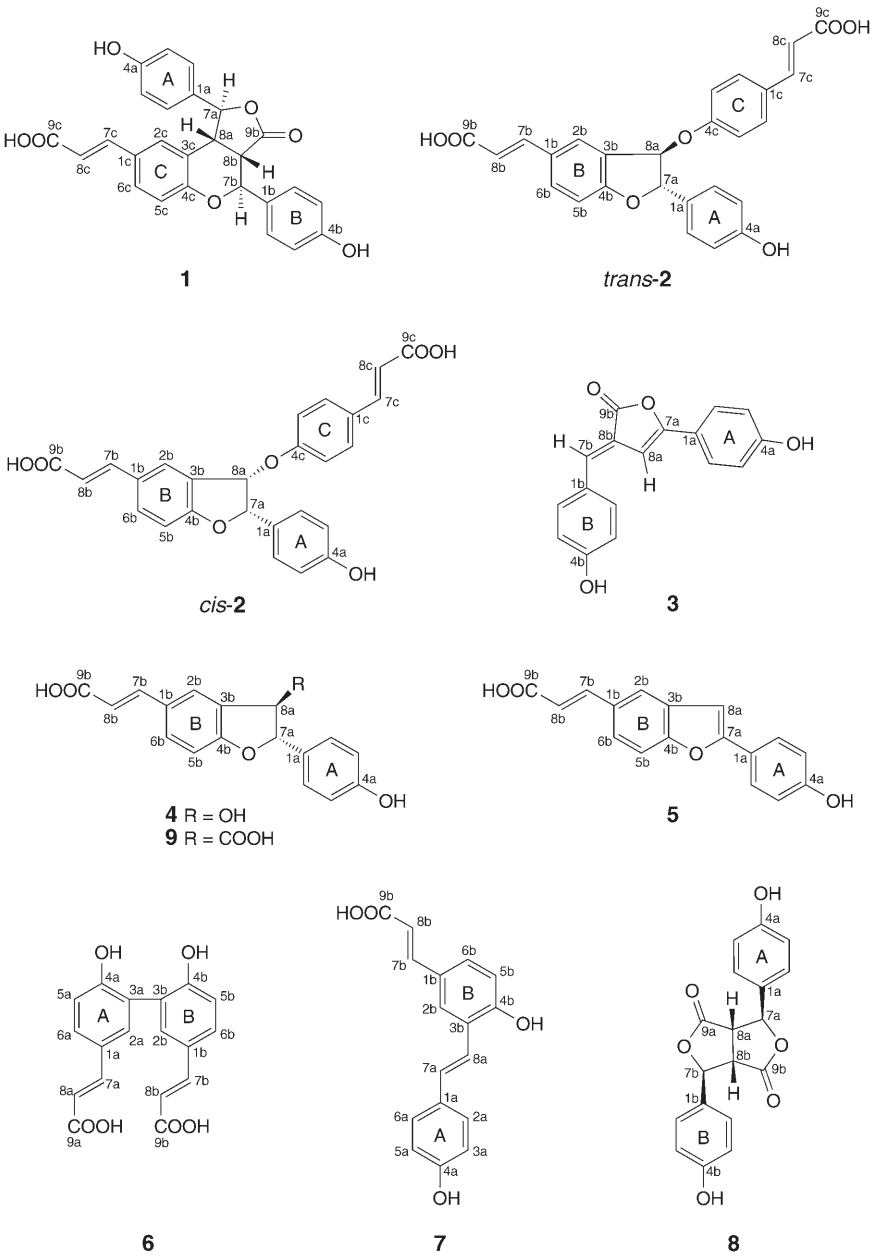

Fig. 1. *Structures of compounds* **1** – **9** *with the applied atom numbering*

compounds and three, diCA5 (**7**), diCA6 (**8**), and diCA7 (**9**) are known compounds, obtained by MCP catalysis *in vitro* for the first time. In the present paper, we report on the biotransformation of CA by MCP guided by means of LC/MS^3, on the di- and trimer isolation and their structural characterization, on the antioxidative activity of seven compounds, *i.e.*, of *trans*-**2**, *cis*-**2**, **3**, and **6**–**9**, as well as on the possible mechanism of formation of **1**–**9**. This is the first report on a successful biotansformation of CA catalyzed by peroxidase *in vitro*.

2. Results and Discussion. – To study the biotransformation of CA by MCP *in vitro* and to further detect the dimer and trimer products of CA, the method of LC/MS^3 was used. We found that the oxidation of CA by MCP led to the formation of the quasimolecular-ion peaks corresponding to didehydro dimers (*m*/*z* 325, 297, and 281), trimers (*m*/*z* 443 and 487), and oligomers (*m*/*z* 563, 585, 561, and 559). We chose biotransformation conditions at different temperatures, different concentrations of H_2O_2, different concentrations of substrate or enzyme, different organic/buffer solvents, and different reaction times in the stable range of MCP and found that the concentration of H_2O_2 significantly influenced the polymerization of CA. Decreasing the H_2O_2 concentration favored the formation of didehydro dimers, and increasing the H_2O_2 concentration favored the formation of trimers and oligomers. A typical HPLC of the product mixture containing 19 peaks is shown in *Fig. 2*. The 19 peaks were assigned by the ESI-MS and MS^3 data, and the retention times t_R compared with the parent CA and ten compounds obtained from the oxidation products of CA (see *Table 1*).

To characterize the major products, the reaction of MCP with CA was carried out under optimal reaction condition guided by LC/MS^3. Ten compounds were isolated from the oxidation mixture of CA by column chromatography on *ODS-C$_{18}$* and *Sephadex LH-20*. On the basis of the physical- and spectroscopic-data analyses, their structures were identified as (2*E*)-3-[*trans*-1-*cisoid*-3a,9b-*trans*-4-1,3a,4,9b-tetrahydro-1,4-bis(4-hydroxyphenyl)-3-oxo-3*H*-furo[3,4-*c*][1]benzopyran-8-yl]prop-2-enoic acid (**1**), (2*E*)-3-{4-{{*trans*-5-[(1*E*)-2-carboxyethenyl]-2,3-dihydro-2-(4-hydroxyphenyl)ben-

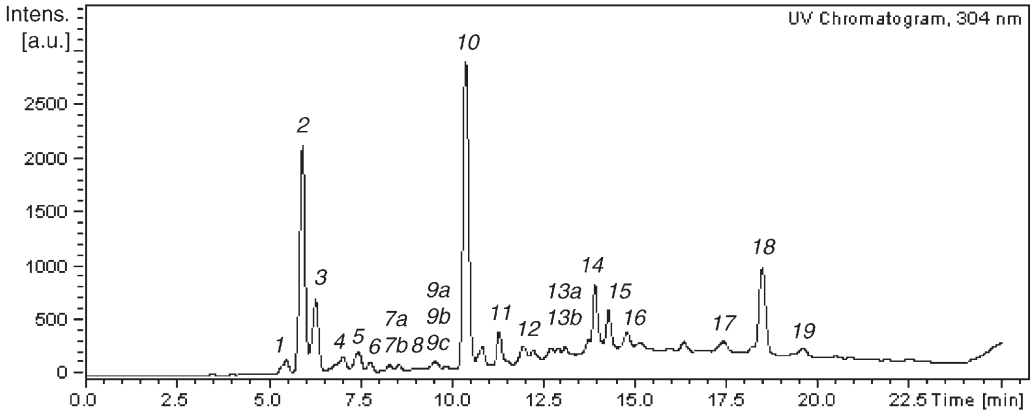

Fig. 2. *The 19 major peaks in the HPLC of the product mixture after CA oxidation by MCP/H_2O_2.* [a.u.] = arbitrary unit.

Table 1. *The LC/MS³ Results of the Oxidation of CA by MCP*

Peak	t_R [min]	Compd.	M_r	MS¹	MS²	MS³
1	5.2–5.4	dimer	326	325 ($[M-H]^-$)	237 ($[M-2\,CO_2-H]^-$)	–
2	5.9–6.0	CA	164	163 ($[M-H]^-$)	119 ($[M-CO_2-H]^-$)	–
3	6.2–6.5	dimer	282	281 ($[M-H]^-$)	237 ($[M-CO_2-H]^-$)	219 ($[M-CO_2-H_2O-H]^-$)
4	6.7–7.1	dimer	298	297 ($[M-H]^-$)	253 ($[M-CO_2-H]^-$)	–
5	7.3–7.7	diCA6 (**8**)	326	325 ($[M-H]^-$)	281 ($[M-CO_2-H]^-$), 237 ($[M-CO_2-H_2O-H]^-$)	237 ($[M-2\,CO_2-H]^-$)
6	7.8–7.9	diCA4 (**6**)	326	325 ($[M-H]^-$)	237 ($[M-2\,CO_2-H]^-$), 281 ($[M-CO_2-H]^-$)	–
7a	8.1–8.4	trimer	444	443 ($[M-H]^-$)	399 ($[M-CO_2-H]^-$)	355 ($[M-2\,CO_2-H]^-$)
7b	8.2–8.4	diCA2 (**4**)	298	297 ($[M-H]^-$)	253 ($[M-CO_2-H]^-$)	235 ($[M-CO_2-H_2O-H]^-$)
8	8.7–9.0	trimer	488	487 ($[M-H]^-$)	469 ($[M-CO_2-H]^-$)	425 ($[M-CO_2-H_2O-H]^-$), 381 ($[M-2\,CO_2-H_2O-H]^-$)
9a	9.0–9.1	trimer	416	415 ($[M-H]^-$)	371 ($[M-CO_2-H]^-$), 343 ($[M-MeCOOH-H]^-$)	–
9b	9.2–9.9	trimer	488	487 ($[M-H]^-$)	399 ($[M-2\,CO_2-H]^-$)	355 ($[M-3\,CO_2-H]^-$)
9c	9.7–9.9	tetramer	586	585 ($[M-H]^-$)	443 ($[M-142-H]^-$)	–
10	10.5–10.6	diCA7 (**9**)	326	325 ($[M-H]^-$)	281 ($[M-CO_2-H]^-$)	237 ($[M-2\,CO_2-H]^-$)
11	10.7–11.5	diCA5 (**7**)	282	281 ($[M-H]^-$)	237 ($[M-CO_2-H]^-$)	–
12	11.8–12.8	triCA1 (**1**)	444	443 ($[M-H]^-$)	399 ($[M-CO_2-H]^-$)	355 ($[M-2\,CO_2-H]^-$)
13a	12.9–13.2	tetramer	562	561 ($[M-H]^-$)	517 ($[M-CO_2-H]^-$)	–
13b	12.9–13.1	trimer	460	459 ($[M-H]^-$)	325 ($[M-134-H]^-$)	281 ($[M-134-CO_2-H]^-$)
14	14.0–14.5	triCA3 (*cis*-**2**)	444	443 ($[M-H]^-$)	399 ($[M-CO_2-H]^-$)	355 ($[M-2\,CO_2-H]^-$)
15	14.7–15.1	diCA1 (**3**)	280	279 ($[M-H]^-$)	251 ($[M-CO_2-H]^-$)	–
16	14.9–15.2	tetramer	562	561 ($[M-H]^-$)	517 ($[M-CO_2-H]^-$)	–
17	17.4–17.5	diCA3 (**5**)	280	279 ($[M-H]^-$)	235 ($[M-CO_2-H]^-$)	–
18	18.3–18.8	triCA2 (*trans*-**2**)	444	443 ($[M-H]^-$)	399 ($[M-CO_2-H]^-$)	355 ($[M-2\,CO_2-H]^-$)
19	19.6–19.8	tetramer	562	561 ($[M-H]^-$)	517 ($[M-CO_2-H]^-$)	–

zofuran-3-yl}oxy}phenyl}prop-2-enoic acid (*trans*-**2**), (2*E*)-3-{4-{{*cis*-5-[(1*E*)-2-carboxyethenyl]-2,3-dihydro-2-(4-hydroxylphenyl)benzofuran-3-yl}oxy}phenyl}prop-2-enoic acid (*cis*-**2**), (3*E*)-5-(4-hydroxyphenyl)-3-[(4-hydroxyphenyl)methylene]furan-2(3*H*)-one (**3**), (2*E*)-3-[*trans*-2,3-dihydro-3-hydroxy-2-(4-hydroxyphenyl)benzofuran-5-yl]-prop-2-enoic acid (**4**), (2*E*)-3-[2-(4-hydroxyphenyl)benzofuran-5-yl]prop-2-enoic acid (**5**), (2*E*,2′*E*)-3,3′-[6,6′-dihydroxy[1,1′-biphenyl]-3,3′-diyl]bis[prop-2-enoic acid] (**6**), (2*E*)-3-[4-hydroxy-3-[(1*E*)-2-(4-hydroxyphenyl)ethenyl]prop-2-enoic acid (**7**), (3α,3aα,6α,6aα)-tetrahydro-3,6-bis(4-hydroxyphenyl)-1*H*,4*H*-furo[3,4-*c*]furan-1,4-dione (**8**), and *trans*-5-[(1*E*)-2-carboxyethenyl]-2,3-dihydro-2-(4-hydroxyphenyl)benzofuran-3-carboxylic acid (**9**). Among them, **1**–**6** are new compounds.

TriCA1 (**1**) was obtained as an optically active amorphous powder. Its molecular formula was determined as $C_{26}H_{20}O_7$ by HR-FAB-MS (*m*/*z* 445.1286 ($C_{26}H_{21}O_7^+$)), indicating a CA trimer. The IR spectrum exhibited absorptions at 3418 (OH), 1747 (C=O, lactone), 1684 (C=O, carbonyl), and 1612 cm^{-1} (phenyl). ^1H- and ^{13}C-NMR (*Table 2*), HSQC, HMBC, and NOESY data established the structure and relative configuration of **1**.

Table 2. *^{1}H- and ^{13}C-NMR Data for TriCA1* (**1**), *TriCA2* (*trans*-**2**), *and TriCA3* (*cis*-**2**)[a])[1]). δ in ppm, J in Hz.

	1[b])		*trans*-**2**[c])		*cis*-**2**[d])	
	δ(H)	δ(C)	δ(H)	δ(C)	δ(H)	δ(C)
C(1a)		129.9		130.3		126.5
H–C(2a,6a)	7.37 (br. *d*, *J* = 8.6)	131.6	7.09 (br. *d*, *J* = 8.6)	128.6	7.31 (br. *d*, *J* = 8.6)	131.2
H–C(3a,5a)	6.90 (br. *d*, *J* = 8.6)	118.2	6.77 (br. *d*, *J* = 8.6)	116.7	6.72 (br. *d*, *J* = 8.6)	115.9
C(4a)		160.8		159.2		158.9
H–C(7a)	5.55 (*d*, *J* = 7.8)	88.2	5.58 (*d*, *J* = 2.4)	91.5	5.89 (*d*, *J* = 6.1)	89.6
H–C(8a)	3.90 (*dd*, *J* = 7.8, 8.0)	44.8	5.94 (*d*, *J* = 2.4)	85.0	6.17 (*d*, *J* = 6.1)	80.0
C(1b)		130.4		129.5		129.5
H–C(2b)	7.27 (br. *d*, *J* = 8.6)	131.6	7.66 (*d*, *J* = 1.9)	127.8	7.89 (*d*, *J* = 1.8)	128.0
H–C(3b)	6.77 (br. *d*, *J* = 8.6)	117.0		127.4		128.9
or C(3b)						
C(4b)		160.3		164.3		163.7
H–C(5b)	6.77 (br. *d*, *J* = 8.6)	117.0	6.95 (*d*, *J* = 8.5)	111.7	7.04 (*d*, *J* = 8.4)	112.0
H–C(6b)	7.27 (br. *d*, *J* = 8.6)	131.6	7.61 (*dd*, *J* = 8.5, 1.9)	133.3	7.70 (*dd*, *J* = 8.4, 1.8)	133.2
H–C(7b)	5.34 (*d*, *J* = 8.8)	75.8	7.63 (*d*, *J* = 15.9)	145.7	7.65 (*d*, *J* = 16.0)	145.6
H–C(8b)	3.51 (*dd*, *J* = 8.8, 8.0)	46.4	6.34 (*d*, *J* = 15.9)	117.4	6.40 (*d*, *J* = 16.0)	117.3
C(9b)		176.1		170.5		168.4
C(1c)		129.9		129.4		129.0
H–C(2c)	6.89 (br. *s*)	131.8	7.53 (br. *d*, *J* = 8.7)	131.0	7.46 (br. *d*, *J* = 8.7)	130.8
C(3c)		123.0	6.96 (br. *d*, *J* = 8.7)	117.7	6.87 (br. *d*, *J* = 8.7)	117.5
or H–C(3c)						
C(4c)		158.6		160.3		160.9
H–C(5c)	6.96 (*d*, *J* = 8.5)	120.4	6.96 (br. *d*, *J* = 8.7)	117.7	6.87 (br. *d*, *J* = 8.7)	117.5
H–C(6c)	7.51 (*dd*, *J* = 8.5, 1.8)	131.8	7.53 (br. *d*, *J* = 8.7)	131.0	7.46 (br. *d*, *J* = 8.7)	130.8
H–C(7c)	7.34 (*d*, *J* = 16.0)	145.9	7.61 (*d*, *J* = 15.9)	145.9	7.53 (*d*, *J* = 16.0)	145.5
H–C(8c)	6.11 (*d*, *J* = 16.0)	119.8	6.31 (*d*, *J* = 15.9)	116.9	6.30 (*d*, *J* = 16.0)	117.3
C(9c)		170.2		170.6		168.4
ArO*H*	9.68, 9.50 (2*s*)		–		–	

[a]) The ^{1}H and ^{13}C signals were assigned by HSQC and HMBC. [b]) 600 (^{1}H) and 150 MHz (^{13}C), in (D_6)DMSO. [c]) 600 (^{1}H) and 150 MHz (^{13}C), in CD_3OD. [d]) 600 (^{1}H) and 150 MHz (^{13}C), in (D_6)acetone.

By ^{1}H-NMR spectroscopy (*Table 2*), the presence of two *p*-disubstituted aromatic fragments **A** and **B** (see *Fig. 1*) were indicated by two *AB* systems (with $J = 8.6$ at δ 7.37 and 6.90 and at δ 7.27 and 6.77, resp.), and a *m*-substituted aromatic fragment **C** was evident by an *AMX* system with ^{1}H-NMR signals at δ 7.51 (*dd*), 6.96 (*d*), and 6.89 (br. *s*). *trans*-Coupling of protons giving rise to the signals at δ 7.34 (*d*, $J =$ 16.0 Hz) and 6.11 (*d*, $J = 16.0$ Hz) revealed an (*E*)-ethenyl group. Vicinal H-atoms at δ 5.55 (*d*, $J =$ 7.8 Hz) and 3.90 (*dd*, $J = 7.8$, 8.0 Hz) as well as at δ 5.34 (*d*, $J = 8.8$ Hz) and 3.51 (*dd*, $J = 8.8$, 8.0 Hz) pointed to two sets of CH–CH fragments in the saturated part of the molecule. Two mobile H-atoms at δ 9.68 and 9.50 were also characterized. A ^{13}C-NMR signal at δ 176.1 (C(9b)) confirmed the presence of a lactone ring. The signals at δ 170.2 (C(9c)), 145.9 (C(7c)), and 119.8 (C(8c)) showed the presence of a propenoic acid side chain[1]). Among the 18 aromatic C-atoms, three with signals at δ 160.8 (C(4a)), 160.3 (C(4b)), and 158.6 (C(4c)) were O-substituted, four with signals at δ 130.4 (C(1b)), 129.9 (C(1a)), 129.9 (C(1c)), and 123.0 (C(3c)) were C-substituted, and the remaining aromatic C-atoms were H-substituted.

[1]) Arbitrary atom numbering; for systematic names, see *Sect. 3* (*Experimental*).

Two nonaromatic oxygenated C-atoms with signals at δ 88.2 (C(7a)) and 75.8 (C(7b)), and two further, C- and H-substituted C-atoms with signals at δ 44.8 (C(8a)) and 46.4 (C(8b)) were also found. HSQC and HMBC measurements led to the following neighborhood relations: H–C(7c)/C(2c) and C(6c), H–C(8c)/C(1c), and H–C(2c) and H–C(6c)/C(7c), suggesting that the disubstituted C(7c)=C(8c) bond (δ(H) 7.34 (H–C(7c)) and 6.11 (H–C(8c))) was connected to the aromatic fragment **C** (*Fig. 1*). The CH(7a)–CH(8a) fragment showed the following correlations: H–C(7a)/C(2a) and C(6a), H–C(2a) and H–C(6a)/C(7a), and H–C(8a)/C(1a), demonstrating that the aromatic fragment **A** was connected to the CH group with the H-signal at δ 5.55 H–C(7a) *via* C(1a). The correlations H–C(7a)/C(8a) and C(9b) and the chemical shift of C(7a) (δ 88.2) indicated that the O-atom of the lactone group was also connected to CH(7a); the correlations H–C(8a)/C(2c) and C(4c), H–C(2c)/C(8a), and H–C(7a)/C(3c) clarified that the CH group at δ 3.90 H–C(8a)) was ^3J(H,C) coupled to C(5c) of the trisubstituted aromatic fragment **C**. The other CH–CH fragment (C(7b)–C(8b)) gave the correlations H–C(7b)/C(2b) and C(6b), H–C(2b)/C(6b) and C(7b), and H–C(8b)/C(1b), supporting that the aromatic fragment **B** was connected to the CH group at δ 5.34 H–C(7b) *via* C(1b). The correlation H–C(7b)/C(4c) and the chemical shift of C(7b) (δ 75.8) indicated that the aromatic fragment **C** was also connected to the CH(7b) group, *via* the 'phenolic' O-atom. The correlations H–C(8b)/H–C(7b) to C(9b) revealed that the CH group at δ 3.51 (H–C(8b)) was connected to the lactone carbonyl group. The two sets of CH–CH groups of the saturated part were connected to each other *via* C(8a)–C(8b), because the correlations H–C(8b)/C(7a), H–C(8a)/C(7b), H–C(7b)/C(8a), H–C(7a)/C(8b), H–C(8a)/C(9b), and H–C(8b)/C(5c) were detected. According to the above analysis, the structure of **1** contained a 1,3a,4,9b-tetrahydro-3*H*-furo[3,4-*c*][1]benzopyran-3-one moiety. The relative configurations of **1** were elucidated by NOESY measurements. The observed NOE correlations H–C(8a)/H–C(2a), H–C(6a), H–C(8b), and H–C(2c), H–C(8b)/H–C(2b), H–C(6b), and H–C(8a), and H–C(7a)/H–C(7b) suggested that the configurations for H–C(7a)/H–C(8a) and H–C(7b)/H–C(8b) should be *trans*, while the configuration for H–C(8a)/H–C(8b) should be *cis*.

TriCA2 (*trans*-**2**) was obtained as an optically active amorphous powder. Its molecular formula was determined as $C_{26}H_{20}O_7$ by HR-FAB-MS (*m*/*z* 445.1288 ($C_{26}H_{21}O_7^+$)), indicating a CA trimer. The IR spectrum exhibited absorptions at 3447 (OH), 1680 (C=O, ester), and 1601 and 1508 cm^{-1} (phenyl). Analysis of the ^{1}H- and ^{13}C-NMR spectrum (*Table 2*) showed that *trans*-**2** contained two disubstituted aromatic fragments **A** and **C**, one trisubstituted aromatic fragment **B**, two disubstituted C=C bonds, a saturated CH–CH fragment, and two carboxylic acid groups (*Fig. 1*). The HSQC experiment established all direct ^{1}H,^{13}C connectivities, and HMBC and NOESY data confirmed the structure of *trans*-**2**.

Key HMBC in *trans*-**2** led to the neighborhood relations H–C(7b)/C(2b) and C(6b), H–C(8b)/C(1b), H–C(2b) and H–C(6b)/C(7b), H–C(7c)/C(2c) and C(6c), H–C(8c)/C(1c), and H–C(2c) and H–C(6c)/C(7c), suggesting that the two disubstituted C=C bonds were connected to aromatic fragments **B** and **C**, respectively. The CH(1a)–CH(7a) moiety showed the correlations H–C(7a)/C(2a) and C(6a), H–C(2a) and H–C(6a)/C(7a), and H–C(8a)/C(1a), demonstrating that the aromatic fragment **A** was connected to the CH group at δ 5.58 (H–C(7a)) *via* C(1a). The correlation H–C(7a)/C(4b) and the chemical shift of C(7a) (δ 91.5) indicated that the aromatic fragment **B** was also connected to the CH(7a) group, *via* the 'phenolic' O-atom. The correlation H–C(8a)/C(4c) and the chemical shift of C(8a) (δ 85.0) revealed that the aromatic fragment **C** was connected to the CH(8a) group, *via* the 'phenolic' O-atom. The correlation H–C(8a)/C(2b) and C(4b) and H–C(2b)/C(8a) indicated that the aromatic fragment **B** was also connected to the CH(8a) group *via* C(3b). According to the above analysis, the structure of *trans*-**2** contained a 2,3-dihydrobenzofuran moiety. The relative configuration of *trans*-**2** was elucidated by NOESY measurements and the coupling constant between H–C(7a) and H–C(8a). The observed NOEs H–C(8a)/H–C(2a), H–C(6a), H–C(3c), and H–C(5c), and H–C(7a)/H–C(2a) and H–C(6a) and the missing of an NOE correlation H–C(7a)/H–C(8a) suggested that the relation for H–C(7a)/H–C(8a) should be *trans*.

TriCA3 (*cis*-**2**) was obtained as an optically active amorphous powder. Its molecular formula was determined as $C_{26}H_{20}O_7$ by HR-FAB-MS (*m/z* 445.1279 ($C_{26}H_{21}O_7^+$)), indicating a CA trimer. The IR spectrum exhibited absorptions at 3441 (OH), 1682 (C=O, ester), and 1605 and 1502 cm^{-1} (phenyl). Analysis of the ^{1}H- and ^{13}C-NMR spectra (*Table 2*) showed that *cis*-**2** contained two disubstituted aromatic fragments, one trisubstituted aromatic fragment, two disubstituted C=C bonds, a CH–CH saturated fragment, and two COOH groups (*Fig. 1*), which indicated that *cis*-**2** should also possess a 2,3-dihydrobenzofuran ring system. Its structure was established by further spectral data.

The 1D- (^{1}H and ^{13}C) and 2D-NMR (HSQC and HMBC) data of *cis*-**2** were very similar to those of *trans*-**2**, except that the coupling constant ^3J(7a,8a) of the saturated CH–CH fragment increased from 2.4 Hz to 6.1 Hz. Comparison of the optical rotations of *cis*- and *trans*-**2** (see *Exper. Part*) indicated that *cis*- and *trans*-**2** should be structural isomers. The NOE correlation H–C(7a)/H–C(8a) and the absence of the correlations H–C(8a)/H–C(2a) and H–C(6a) suggested the relative *cis*-configuration for H–C(7a)/H–C(8a) in *cis*-**2**, in contrast to the *trans*-configuration in *trans*-**2**.

DiCA1 (**3**) was obtained as a red powder. Its molecular formula was determined as $C_{17}H_{12}O_4$ by HR-ESI-MS (*m/z* 281.0801 ($C_{17}H_{13}O_4^+$)), which indicated a product formed by didehydrodimerization of CA. The IR spectrum exhibited absorptions at 3433 (OH), 1632 (C=C), and 1595 cm^{-1} (phenyl). Analysis of the ^{1}H- and ^{13}C-NMR spectra (*Table 3*) showed that **3** contained two disubstituted aromatic fragments **A** and **B**, two tri-substituted C=C bonds, and one C=O group (*Fig. 1*). HSQC and HMBC Experiments established all ^1J and ^3J ^{1}H,^{13}C connectivities and allowed to combine these partial structures to that of **3**. Finally, NOE experiments established the configuration of the exocyclic C=C bond of **3**.

The 3-methylenefuran-2(3*H*)-one moiety of **3** was unambiguously assigned by the correlations H–C(8a)/C(7b), C(8b), and C(9b) and H–C(7b)/C(8a), C(8b), and C(9b). The correlations H–C(2a) and H–C(6a)/C(7a), and H–C(8a)/C(1a) as well as the correlations H–C(2b) and H–C(6b)/C(7b), H–C(7b)/C(2b) and C(6b) established that the aromatic fragment **A** was connected to C(7a) and the aromatic fragment **B** to C(7b) of the 3-methylenefuran-2(3*H*)-one moiety, *via* C(1a) and C(1b), resp. The configuration at the exocyclic C=C bond was determined to be (*E*) by the NOE effect H–C(8a)/H–C(6b).

DiCA2 (**4**) was obtained as an optically active amorphous powder. Its molecular formula was determined as $C_{17}H_{14}O_5$ by HR-ESI-MS (*m/z* 297.0773 ($C_{17}H_{13}O_5^-$)), indicating the presence of a second didehydrodimerization product of CA. The IR spectrum exhibited absorptions at 3418 (OH), 1684 (C=O, ester), and 1610 and 1502 cm^{-1} (phenyl). Analysis of the ^{1}H- and ^{13}C-NMR spectra (*Table 3*) showed that **4** contained one disubstituted aromatic fragment **A** and one trisubstituted aromatic fragment **B**, one disubstituted C=C bond, one CH–CH fragment, linked to two O-functions, and a COOH group (*Fig. 1*). Further NMR experiments confirmed the proposed structure of **4**.

The HSQC experiment with **4** established all C–H bonds. HMBC Measurements revealed the correlations H–C(7a) and H–C(8a)/C(4b) and H–C(2b)/C(8a), supporting the fact that the 2,3-dihydrobenzofuran structure was composed of the aromatic fragment **B**, the 'phenolic' OH group, and the CH–CH fragment. The correlations H–C(7b)/C(2b) and C(6b), H–C(8b)/C(1b), and H–C(2b)

Table 3. *^{1}H- and ^{13}C-NMR Data for DiCA1* (**3**), *DiCA2* (**4**), *DiCA3* (**5**), *and DiCA4* (**6**)[a])[1]). δ in ppm, J in Hz.

	3[b])		**4**[c])		**5**[d])		**6**[c])	
	δ(H)	δ(C)	δ(H)	δ(C)	δ(H)	δ(C)	δ(H)	δ(C)
C(1a)		128.5		130.6		122.3		127.5
H–C(2a)	7.72 (br. d, J = 8.8)	128.4	7.15 (br. d, J = 8.6)	127.0	7.77 (br. d, J = 8.7)	128.4	7.45 (d, J = 2.2)	130.0
H–C(3a)	6.95 (br. d, J = 8.8)	117.5	6.78 (br. d, J = 8.6)	115.4	6.90 (br. d, J = 8.7)	117.7		127.1
C(4a)		160.8		157.7		160.4		158.2
H–C(5a)	6.95 (br. d, J = 8.8)	117.5	6.78 (br. d, J = 8.6)	115.4	6.90 (br. d, J = 8.7)	117.7	7.48 (dd, J = 8.4, 2.2)	117.5
H–C(6a)	7.72 (br. d, J = 8.8)	128.4	7.15 (br. d, J = 8.6)	127.0	7.77 (br. d, J = 8.7)	128.4	6.93 (d, J = 8.4)	133.2
C(7a)		157.3	5.40 (d, J = 4.0)	93.2		158.9	7.64 (d, J = 15.9)	146.5
or H–C(7a)								
H–C(8a)	7.20 (s)	99.3	5.18 (d, J = 4.0)	79.1	7.21 (s)	101.2	6.31 (d, J = 15.9)	116.0
C(9a)		–		–		–		170.9
C(1b)		121.5		128.3		131.4		127.5
H–C(2b)	7.71 (br. d, J = 8.8)	133.8	7.67 (d, J = 1.9)	125.8	7.93 (br. s)	122.8	7.45 (d, J = 2.2)	130.0
H–C(3b)	6.94 (br. d, J = 8.8)	117.2		130.0		131.7		127.1
or C(3b)								
C(4b)		160.9		162.6		156.8		158.2
H–C(5b)	6.94 (br. d, J = 8.8)	117.2	6.94 (d, J = 8.4)	110.4	7.62 (br. s)	113.1	7.48 (dd, J = 8.4, 2.2)	117.5
H–C(6b)	7.71 (br. d, J = 8.8)	133.8	7.57 (dd, J = 8.4, 1.9)	131.5	7.62 (br. s)	126.0	6.93 (d, J = 8.4)	133.2
H–C(7b)	7.21 (s)	134.7	7.68 (d, J = 15.9)	145.2	7.71 (d, J = 15.9)	146.3	7.64 (d, J = 15.9)	146.5
H–C(8b)		123.7	6.37 (d, J = 15.9)	115.4	6.53 (d, J = 15.9)	119.7	6.31 (d, J = 15.9)	116.0
C(9b)		170.7		169.9		169.5		170.9
Ar*O*H	–		–		9.91		–	
COOH	–		–		12.31		–	

[a]) The ^{1}H and ^{13}C signals were assigned by HSQC and HMBC. [b]) 600 (^{1}H) and 150 MHz (^{13}C), in (D_6)acetone. [c]) 600 (^{1}H) and 150 MHz (^{13}C), in CD_3OD. [d]) 600 (^{1}H) and 150 MHz (^{13}C), in (D_6)DMSO.

and H–C(6b)/C(7b) suggested that the disubstituted C=C bond, with the olefinic H-atoms at δ 7.68 (H–C(7b)) and 6.37 (H–C(8b)), was connected to C(1b) of the dihydrobenzofuran. The correlations H–C(7a)/C(2a) and C(6a), H–C(2a) and H–C(6a)/C(7a), and H–C(8a)/C(1a) suggested that the aromatic fragment **A** was connected to the CH(7a) group at δ 5.40 of the dihydrobenzofuran, *via* C(1a). The chemical shifts of H–C(8a) (δ(C) 79.1, δ(H) 5.18) of the dihydrobenzofuran moiety established that an OH group was also connected to C(8a). The NOE correlations H–C(8a)/H–C(2a) and H–C(6a) and the missing NOE H–C(8a)/H–C(7a) supported the conclusion that the spatial relation of H–C(7a)/H–C(8a) should be *trans*.

DiCA3 (**5**) was obtained as an amorphous powder. Its molecular formula was determined as $C_{17}H_{12}O_4$ by HR-ESI-MS (*m/z* 281.0803 ($C_{17}H_{13}O_4^+$)), indicating a didehydrodimerization product of CA. The IR spectrum exhibited absorptions at 3427 (OH), 1678 (C=O, ester), and 1618 and 1501 cm^{-1} (phenyl). Analysis of the ^{1}H- and ^{13}C-NMR spectra (*Table 3*) showed that **5** contained one disubstituted aromatic fragment **A** and one trisubstituted aromatic fragment **B**, one disubstituted C=C bond, one trisubstituted C=C bond, and one COOH group (*Fig. 1*). Further spectral data established the structure of **5**.

The ^{1}H- and ^{13}C-NMR spectra of **5** were very similar to those of **4**, except that the signals of H–C(7a) at δ 5.40 (*d*, J = 4.0 Hz) and H–C(8a) at δ 5.18 (*d*, J = 4.0 Hz) of the saturated moiety of **4** were no longer present, while an additional signal of an olefinic proton at δ 7.21 (*s*) was observed, and the signals of C(7a) and C(8a) were shifted downfield to δ 158.9 and 101.2 as compared to those of **4** at δ 93.2 and 79.1, indicating unequivocally the presence of a benzofuran moiety. The assignment of the signals in the ^{1}H- and ^{13}C-NMR spectra (*Table 3*) is based on the detailed analysis of the splitting pattern and of HSQC and HMBC plots.

DiCA4 (**6**) was obtained as a yellow powder. Its molecular formula was determined as $C_{18}H_{14}O_6$ by HR-ESI-MS (*m/z* 349.0695 ($C_{18}H_{14}O_6Na^+$)), indicating a didehydrodimerization product of CA. The IR spectrum exhibited absorptions at 3431 (OH), 1684 (C=O, ester), and 1597 and 1499 cm^{-1} (phenyl). The structure of **6** was deduced from the detailed analysis of the ^{1}H- and ^{13}C-NMR data (*Table 3*).

The ^{1}H-NMR spectrum of **6** showed one *AMX* system due to a 1,3,4-trisubstituted aromatic fragment for which the signals were at δ 7.45 (*d*), 6.93 (*d*), and 7.48 (*dd*) in the aromatic region, and an (*E*)-ethenyl group for which the signals were at δ 7.64 (*d*, J = 15.9 Hz) and 6.31 (*d*, J = 15.9 Hz). The ^{13}C-NMR data indicated that **6** possessed a C=O group, an (*E*)-ethenyl group, an O-substituted sp^2 C-atom, two C-substituted sp^2 C-atoms, and three sp^2 CH groups. Only 7 of 14 H-atoms and 9 of 18 C-atoms were observed, suggesting a symmetrical structure for **6**. Furthermore, according to the radical formation by the enzyme, we concluded that radical recombination at the *ortho*-position with respect to the phenolic OH group of the parent CA had taken place.

DiCA5 (**7**) was obtained as a yellow amorphous powder. Its molecular formula was determined as $C_{17}H_{14}O_4$ by ESI-MS in combination with ^{1}H- and ^{13C}-NMR spectral data, indicating a didehydrodimerization product of CA. The structure of **7** was assigned by comparing its ^{1}H- and ^{13}C-NMR spectra with literature data [17][18].

DiCA6 (**8**) was obtained as an optically active white amorphous powder. Its molecular formula was determined as $C_{18}H_{14}O_6$ by ESI-MS in combination with ^{1}H- and ^{13}C-NMR spectral data, indicating a didehydrodimerization product of CA. The structure of **8** was assigned by comparing its ^{1}H- and ^{13}C-NMR spectra with literature data [19].

DiCA7 (**9**) was obtained as an optically active yellow amorphous powder. Its molecular formula was determined as $C_{18}H_{14}O_6$ by ESI-MS in combination with ^{1}H-and ^{13}C-NMR data, indicating a didehydrodimerization product of CA. The structure of **9** was assigned by comparing its ^{1}H- and ^{13}C-NMR spectra with literature data [16].

3. Experimental. – 3.1. *General*. Column chromatography (CC): *Sephadex-LH-20* (20–100 μ; *Pharmacia*) and *ODS-C_{18}* (100–200 μ; *Waters*) columns, *Agilent-Technologies 1100* liquid chromatographe (Wilmington, DE) with binary pump, degasser, autosample, and diode-array detector, coupled online to an ion-trap mass spectrometer interfaced with ESI, controlled by HP1100-ChemStation data software; *Agilent Extend-C_{18}* (2.1 mm × 150 mm; 5 μm) column from *Waters* and H_2O/MeOH gradient (50 → 100% MeOH in 25 min) at a flow rate of 1.0 ml/min at 25° column temp., UV detection at 304 nm, FT-MS in the neg. mode, mass scan from *m*/*z* 50–700. Optical rotations: *Jasco P-1020* digital polarimeter; cell length 1.0 dm. UV Spectra: *Shimadzu UV-2501PC* spectrometer. IR Spectra: *Nicolet Impact-410* spectrometer; in cm^{-1}. ^{1}H- and ^{13}C-NMR, HSQC, HMBC, and NOESY: *Bruker ACF-600*-MHz spectrometer; $SiMe_4$ as an internal standard; chemical shifts δ in ppm, *J* in Hz. HR-FAB-MS: *Jeol HX-110* spectrometer, with 3-nitrobenzyl alcohol as a matrix. HR-ESI-MS: *Agilent TOF-MSD-1946D* spectrometer.

3.2. *Plant Material*. Fruits of *M. charantia* were collected at a suburb of Nanjing, China, and identified by Dr. *Mingjian Qin*, China Pharmaceutical University. A voucher (No. 000804) was deposited in the Department of Natural Medicinal Chemistry, China Pharmaceutical University.

3.3. *Purification of MCP*. MCP from fruits of *Momordica charantia* was purified to electrophoretic homogeneity, in turn by ammonium sulfate fractionation, ion-exchange chromatography (*DEAE-Sepharose FF*), affinity chromatography (*Con A Sepharose*), and gel filtration (*Sephadex G-150*). The detailed method of the purification of MCP was reported previously [1]. The purified MCP exhibited a specific activity of 7757 E.U. of peroxidase per mg of protein, which was 46-fold higher than that of the crude extract.

3.4. *LC/MS^3-Guided Biotransformation of CA in Aqueous Acetone by MCP*. For anal. LC/MS^3, biotransformation of CA (10 mg) in acetone (1 ml) was performed with a soln. of MCP (80 U) in AcONa buffer (500 mM, 4.8 ml), pH 5.0, and varying concentrations of H_2O_2 at 45°, which was added dropwise at 1 min intervals in a total reaction volume of 6 ml and stirred for 8 h, during which the mixture was gradually turned flavovirens. The acetone was removed and the aq. mixture extracted with three volumes of AcOEt. The extract was washed with H_2O, dried (Na_2SO_4), and concentrated at 40°. The dried mixture was then redissolved in MeOH (1 ml) for LC/ESI-MS^3 analysis (*Fig. 2*). According to the LC/ESI-MS^3 analysis, all the biotransformation products could easily be found, including the types of the compounds (*Table 1*). With the guide of LC/ESI-MS^3 analysis, systemic isolation could be achieved.

To purify and identify the oxidation products, the reaction was carried out on a large scale. A soln. of CA (1 g) in acetone (40 ml) and a soln. of MCP ($8 \cdot 10^3$ U) in buffer (500 mM AcONa/AcOH, pH 5.0, 85 ml) were mixed and treated with hydrogen peroxidase (3%, 2.5 ml) at 45°, which was added in aliquots at 1 min intervals and stirred for 8 h. Reaction products were extracted with three volumes of AcOEt, and the extract was evaporated at 40°: brown powder (0.9 g), which was subjected to CC (*ODS-C_{18}*, MeOH/H_2O 3:7 → 6:4): *Fractions I–IV*. All the fractions were analyzed by HPLC to find the target products before they were subjected to CC (*Sephadex LH-20*). *Fr. II* (0.5 g from 300 ml, MeOH/H_2O 4:6) was subjected to CC (*Sephadex LH-20*, MeOH, $CHCl_3$/MeOH 1:1, acetone): diCA2 (**4**; 7.5 mg), diCA4 (**6**; 58.5 mg), diCA5 (**7**; 43 mg), diCA6 (**8**; 15 mg), and diCA7 (**9**; 63.5 mg). *Fr. III* (0.3 g from 300 ml, MeOH/H_2O 5:5) was subjected to CC (*Sephadex LH-20*, MeOH, $CHCl_3$/MeOH 1:1, acetone): triCA1 (**1**; 9 mg), triCA3 (*cis*-**2**; 12.3 mg), diCA1 (**3**; 37.2 mg), and diCA3 (**5**; 8.5 mg). *Fr. IV* (0.1 g from 300 ml, MeOH/H_2O 6:4) was subjected to CC (*Sephadex LH-20*, MeOH, $CHCl_3$/MeOH 1:1): triCA2 (*trans*-**2**; 16.7 mg). With the guide of LC/ESI-MS^3, it was easy to find out that the main products of biotransformation had been obtained.

TriCA1 (= rel-*(2*E*)-3-[(1*R*,3a*R*,4*R*,9b*S*)-1,3a,4,9b-Tetrahydro-1,4-bis(4-hydroxyphenyl)-3-oxo-3*H*-furo[3,4-*c*][1]benzopyran-8-yl]prop-2-enoic Acid*; **1**): White amorphous powder. $[\alpha]_D^{20} = +3.8$ (*c* = 0.12, MeOH). IR (KBr): 3418, 1747, 1684, 1622, 1612, 1242, 1126, 999, 839. ^{1}H-NMR (600 MHz,

(D_6)DMSO) and ^{13}C-NMR (150 MHz, (D_6)DMSO): *Table 2*. HR-ESI-MS (pos.): 445.1286 ($C_{26}H_{21}O_7^+$, $[M+H]^+$; calc. 445.1287).

TriCA2 (= rel-*(2*E*)-3-[4-{{(2*R*,3*S*)-5-[(1*E*)-2-Carboxyethenyl]-2,3-dihydro-2-(4-hydroxyphenyl)-benzofuran-3-yl}oxy}phenyl]prop-2-enoic Acid*; *trans*-**2**): White amorphous powder. $[\alpha]_D^{20} = -0.8$ (c = 0.24, MeOH). IR (KBr): 3447, 3029, 2949, 2928, 1680, 1601, 1508, 1234, 1177, 1117, 970, 831. ^{1}H-NMR (600 MHz, CD_3OD) and ^{13}C-NMR (150 MHz, CD_3OD): *Table 2*. HR-FAB-MS (pos.): 445.1288 ($[M+H]^+$, $C_{26}H_{21}O_7^+$; calc. 445.1287).

TriCA3 (= rel-*(2*E*)-3-[4-{{(2*R*,3*R*)-5-[(1*E*)-2-Carboxyethenyl]-2,3-dihydro-2-(4-hydroxyphenyl)-benzofuran-3-yl}oxy}phenyl]prop-2-enoic Acid*; *cis*-**2**): White amorphous powder. $[\alpha]_D^{20} = +4.0$ (c = 0.15, MeOH). IR (KBr): 3441, 1682, 1605, 1502, 1242, 1173, 1121, 980, 825. ^{1}H-NMR (600 MHz, (D_6)acetone) and ^{13}C-NMR (150 MHz, (D_6)acetone): *Table 2*. HR-FAB-MS (pos.): 445.1279 ($[M+H]^+$, $C_{26}H_{21}O_7^+$; calc. 445.1287).

DiCA1 (= *(3*E*)-5-(4-Hydroxyphenyl)-3-[(4-hydroxyphenyl)methylene]furan-2(3*H*)-one*; **3**). Red amorphous powder. IR (KBr): 3437, 1745, 1610, 1506, 1452, 1254, 1169, 822. ^{1}H-NMR (600 MHz, (D_6)acetone) and ^{13}C-NMR (150 MHz, (D_6)acetone): *Table 3*. HR-ESI-MS (pos.): 281.0801 ($[M+H]^+$, $C_{17}H_{13}O_4^+$; calc. 281.0808).

DiCA2 (= rel-*(2*E*)-3-(2*R*,3*S*)-2,3-Dihydro-3-hydroxy-2-(4-hydroxyphenyl)benzofuran-5-yl]prop-2-enoic Acid*; **4**): White amorphous powder. IR (KBr): 3418, 1684, 1607, 1516, 1487, 1238, 1215, 1122, 821. ^{1}H-NMR (600 MHz, CD_3OD) and ^{13}C-NMR (150 MHz, CD_3OD): *Table 3*. HR-ESI-MS (neg.): 297.0773 ($[M-H]^-$, $C_{17}H_{13}O_5^-$; calc. 297.0768).

DiCA3 (= *(2*E*)-3-[2-(4-Hydroxyphenyl)benzofuran-5-yl]propenoic Acid*; **5**): White amorphous powder. IR (KBr): 3427, 1678, 1618, 1501, 1470, 1225, 982, 814. ^{1}H-NMR (600 MHz, (D_6)DMSO) and ^{13}C-NMR (150 MHz, (D_6)DMSO): *Table 3*. HR-ESI-MS (pos.): 281.0803 ($[M+H]^+$, $C_{17}H_{13}O_4^+$; calc. 281.0808).

DiCA4 (= *(2*E*,2′*E*)-[6,6′-Dihydroxy[1,1′-biphenyl]-3,3′-diyl]bis[prop-2-enoic Acid]*; **6**). White amorphous powder. IR (KBr): 3431, 3061, 3032, 1684, 1622, 1597, 1499, 1427, 1286, 1209, 986, 818. ^{1}H-NMR (600 MHz, CD_3OD) and ^{13}C-NMR (150 MHz, CD_3OD): *Table 3*. HR-ESI-MS (pos.): 349.0695 ($[M+Na]^+$, $C_{18}H_{14}NaO_6^+$; calc. 349.0688).

DiCA5 (= *(2*E*)-3-[4-Hydroxy-3-[(1*E*)-2-(4-hydroxyphenyl)ethenyl]prop-2-enoic Acid*; **7**): Yellow amorphous powder. IR (KBr): 3443, 3373, 1655, 1595, 1506, 1431, 1323, 1254, 1205, 1103, 968. ^{1}H-NMR (600 MHz, (D_6)acetone)[1]: 9.12, 8.47 (2 br. *s*, each 1 H, 2 ArO*H*); 7.93 (br. *s*, H−C(2b)); 7.63 (*d*, *J* = 15.9, H−C(7b)); 7.44 (br. *d*, *J* = 8.7, H−C(2a), H−C(6a)); 7.40 (br. *d*, *J* = 8.4, H−C(6b)); 7.31 (br. *s*, H−C(7a), H−C(8a)); 6.94 (*d*, *J* = 8.4, H−C(5b)); 6.84 (br. *d*, *J* = 8.7, H−C(3a), H−C(5a)); 6.41 (*d*, *J* = 15.9, H−C(8b)). ^{13}C-NMR (150 MHz, (D_6)acetone)[1]: 168.7 (C(9b)); 158.6 (C(4a)); 157.9 (C(4b)); 146.2 (C(7b)); 131.0 (C(1a)); 130.7 (C(7a)); 129.5 (C(6b)); 129.2 (C(2a), C(6a)); 127.9 (C(1b)); 127.8 (C(2b)); 126.9 (C(3b)); 121.1 (C(8a)); 117.5 (C(5b)); 116.9 (C(3a), C(5a)); 116.6 (C(8b)). ESI-MS (neg.): 281 ($[M-H]^-$).

DiCA6 (= rel-*(3*R*,3a*R*,6*R*,6a*R*)-Tetrahydro-3,6-bis(4-hydroxyphenyl)-1*H*,4*H*-furo[3,4-*c*]furan-1,4-dione*; **8**): White amorphous powder. $[\alpha]_D^{20} = +3.0$ (c = 0.10, MeOH). IR (KBr): 3369, 1780, 1753, 1616, 1520, 1236, 1173, 1034, 1016, 993, 831. ^{1}H-NMR (600 MHz, (D_6)acetone)[1]: 7.31 (br. *d*, *J* = 9.5, H−C(2a), H−C(6a), H−C(2b), H−C(6b)); 6.88 (br. *d*, *J* = 9.5, H−C(3a), H−C(5a), H−C(3b), H−C(5b)); 5.77 (*s*, H−C(7a), H−C(7b)); 4.04 (*s*, H−C(8a), H−C(8b)). ^{13}C-NMR (150 MHz, (D_6)acetone)[1]: 176.4 (C(9a), C(9b)); 159.5 (C(4a), C(4b)); 130.9 (C(1a), C(1b)); 128.8 (C(3a), C(3b), C(5a), C(5b)); 117.0 (C(2a), C(2b), C(6a), C(6b)); 83.6 (C(7a), C(7b)); 49.6 (C(8a), C(8b)). ESI-MS (neg.): 325 ($[M-H]^-$).

DiCA7 (= rel-*(2*R*,3*R*)-5-[(1*E*)-2-Carboxyethenyl]-2,3-dihydro-2-(4-hydroxyphenyl)benzofuran-3-carboxylic Acid*; **9**): Yellow amorphous powder. $[\alpha]_D^{20} = -1.6$ (c = 0.23, MeOH). IR (KBr): 3466, 1701, 1680, 1628, 1603, 1518, 1487, 1242, 1115, 980, 825. ^{1}H-NMR (600 MHz, CD_3OD)[1]: 7.63 (br. *s*, H−C(2b)); 7.63 (*d*, *J* = 15.9, H−C(7b)); 7.47 (br. *d*, *J* = 8.4, H−C(6b)); 7.18 (br. *d*, *J* = 8.5, H−C(2a), H−C(6a)); 6.85 (*d*, *J* = 8.4, H−C(5b)); 6.77 (br. *d*, *J* = 8.5, H−C(3a), H−C(5a)); 6.31 (*d*, *J* = 15.9, H−C(8b)); 5.97 (*d*, *J* = 7.1, H−C(7a)); 4.24 (*d*, *J* = 7.1, H−C(8a)). ^{13}C-NMR (150 MHz, CD_3OD)[1]: 178.9 (C(9a)); 169.8 (C(9b)); 161.7 (C(4b)); 157.9 (C(4a)); 145.3 (C(7b)); 131.5 (C(1a)); 130.8 (C(6b));

128.1 (C(1b)); 127.4 (C(2a), C(6a)); 126.6 (C(3b)); 125.1 (C(2b)); 115.5 (C(3a), C(5a), C(8b)); 109.9 (C(5b)); 87.5 (C(7a)); 55.4 (C(8a)). ESI-MS (neg.): 325 ($[M-H]^-$).

3.5. *Antioxidant Activity.* The MDA test kit (No. 20050411) was obtained from *Nanjing JianCheng Biological Engineering Institute.* L-Cysteine hydrochloride was obtained in subpackage from *Amresco.* The antioxidative activity of *trans*-**2**, *cis*-**2**, **3**, and **6**–**9** was tested by the reported methods [20].

The antioxidative activities of *trans*-**2**, *cis*-**2**, **3**, and **6**–**9**, isolated from the oxidation of *p*-coumaric acid were tested *in vitro* by microassay for the measurement of antilipid peroxidation based on the mode of the formation of microsomal lipid peroxidation induced by Fe^{2+}/cysteine. Accordingly, triCA3 (*cis*-**2**), diCA1 (**3**), diCA5 (**7**), and diCA7 (**9**) are stronger antioxidants than CA itself as shown by the inhibition ratio (*Table 4*).

Table 4. *The Inhibition Ratio*[a]) *of the Subjects to MDA*

	Final concentration [mol/l]	Mean ± s.d. [%]
CA	$1 \cdot 10^{-4}$	47.2 ± 4.0
trans-**2**	$1 \cdot 10^{-4}$	37.9 ± 3.4
cis-**2**	$1 \cdot 10^{-4}$	53.8 ± 5.0
3	$1 \cdot 10^{-4}$	65.9 ± 2.1
6	$1 \cdot 10^{-4}$	38.2 ± 3.3
7	$1 \cdot 10^{-4}$	64.5 ± 2.6
8	$1 \cdot 10^{-4}$	44.1 ± 6.0
9	$1 \cdot 10^{-4}$	51.4 ± 2.7

[a]) The inhibition ratio was defined by the following equation: inhibition ratio = (absorbance of vehicle – absorbance of tested compound)/absorbance of vehicle × 100%.

4. Conclusion. – A novel peroxidase (*Momordica charantia* peroxidase, MCP) was purified from the fruit of *Momordica charantia*. We applied the purified MCP as catalyst in the presence of H_2O_2 to the transformation of *p*-coumaric acid (CA). To investigate the effects of H_2O_2 on the di-, tri-, and oligomerization of CA, a control experiment was conducted that showed that H_2O_2 cannot catalyze the CA transformations in the absence of MCP. Guided by the LC/MS^3 analysis, we found that the biotransformation of CA catalyzed by MCP can generate numerous oxidation products including CA dimers, trimers, and oligomers. The H_2O_2 concentration can influence the transformation of CA. With an increasing H_2O_2 concentration, the formation of higher oligomers (quasimolecular-ion peaks at *m*/*z* 563, 585, 561, 559, and so on) can be caused in certain instances.

During our further research, three novel trimers, four novel dimers, and three known dimers were identified from the MCP-catalyzed oxidation of CA. This is the first time that CA trimers and dimers were identified from a peroxidase-catalyzed oxidation of *p*-coumaric acid *in vitro*, and the formation of CA trimers appeared to be favored by the decarboxylation of didehydrodimer intermediates. The proposed reaction mechanism for the formation of the trimer triCA1 (**1**) is shown in *Scheme 1*. It is reasonable to assume that, of the CA radicals **a**–**c**, the mesomers **b** and **c** combine (→ I(1)), followed by acid/base-catalyzed decarboxylation, driven by aromatization of the quinomethane part, to yield diCA5 (**7**). Then, the attack of the monomeric CA radical **b** on the ethenyl bond of **7**, followed by MCP/H_2O_2 catalysis, leads to I(2). Through an intramolecular rearrangement, catalyzed by acid/base, triCA1 (**1**) is formed from I(2).

Scheme 1. *Proposed Mechanism of the Formation of TriCA1* (**1**)

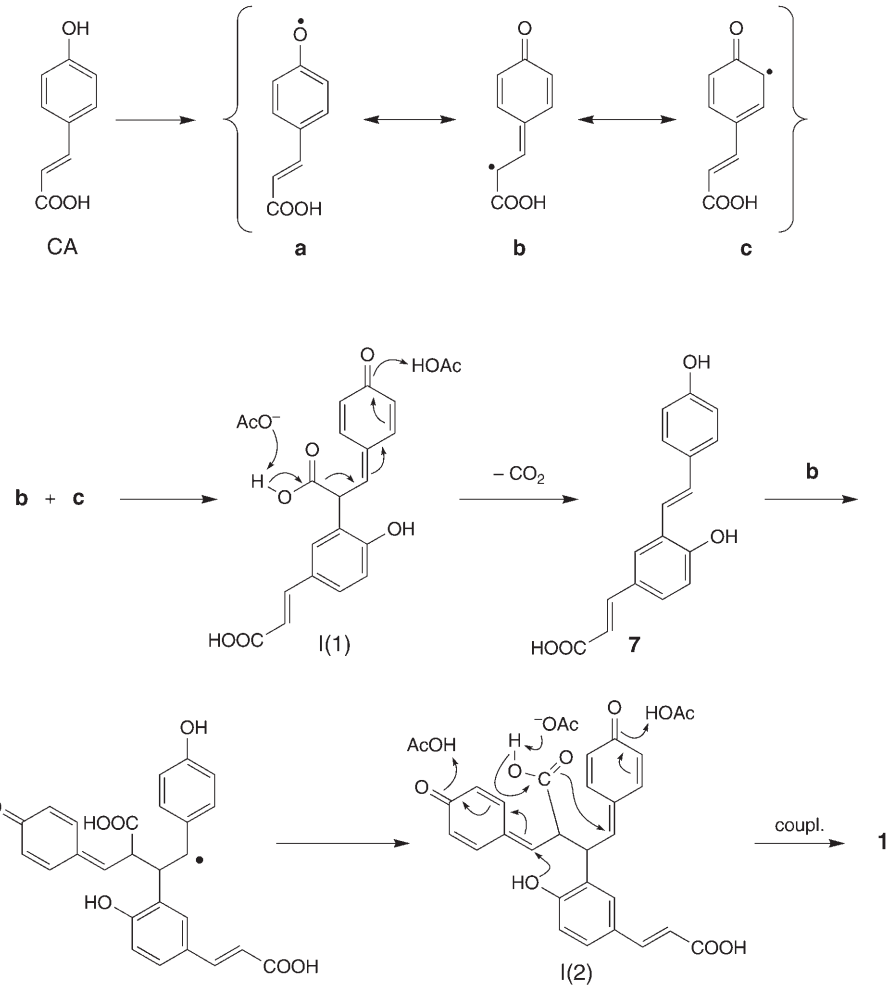

The trimers triCA2 (*trans*-**2**) and triCA3 (*cis*-**2**) also contain a decarboxylated moiety. A possible mechanism of their formation involves the combination of the CA radicals **a** and **b** (→ I(3)), followed by decarboxylation, to yield I(4) (*Scheme 2*). Then, the attack of CA radical **c** on the ethenyl bond of I(4), followed by MCP/H_2O_2 catalysis, leads to I(5). Through an intramolecular rearrangement, catalyzed by acid, triCA2 (*trans*-**2**) and triCA3 (*cis*-**2**) are formed from I(5).

The dimers, diCA1 to diCA7 (**3**–**9**), represent products of 8–8, 8–3, and 3–3 radical coupling, and the possible formation mechanism is shown in *Scheme 3*. Compound **7** is oxidized by MCP/H_2O_2, followed by acid/base catalysis to yield, by intramolecular rearrangement, compound **4**. The intermediate I(1) (see *Scheme 1*), catalyzed by acid, undergoes an intramolecular rearrangement to yield diCA7 (**9**).

Scheme 2. *Proposed Mechanism of the Formation of TriCA2* (*trans*-**2**) *and TriCA3* (*cis*-**2**)

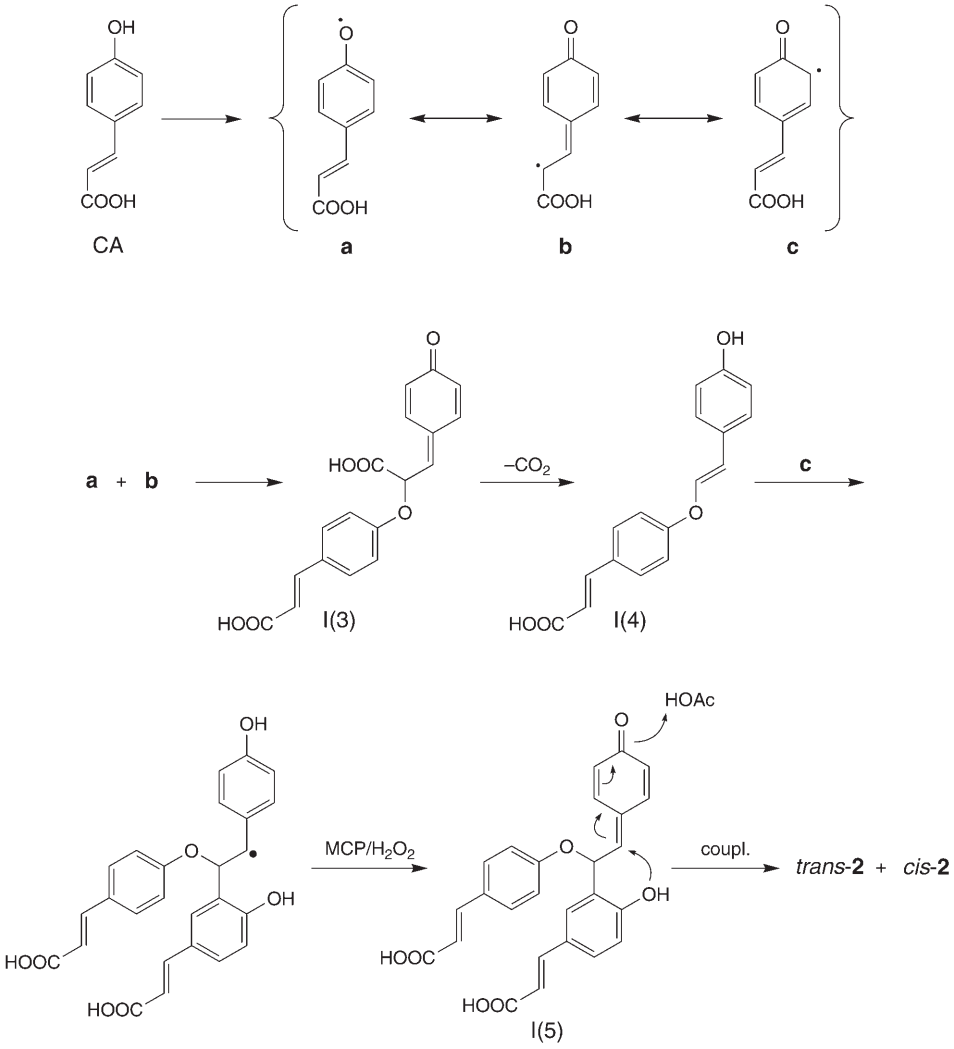

Compound **9** is oxidized by MCP/H_2O_2, followed by acid/base catalysis and decarboxylation, to yield diCA3 (**5**). After combination of the CA radicals **b** (→ I(6)), followed by acid/base-catalyzed decarboxylation, an intramolecular rearrangement yields I(7). The latter is oxidized by MCP/H_2O_2, followed by decarboxylation, to yield diCA1 (**3**). DiCA6 (**8**) is formed from I(7) by intramolecular rearrangement. The 3–3 didehydrodimer appears to result from the combination of two CA radicals **c** to form the corresponding intermediate, which then undergoes deprotonation/aromatization, giving diCA4 (**6**).

Scheme 3. *Proposed Mechanism of the Formation of DiCA1 – DiCA7* (**3** – **9**)

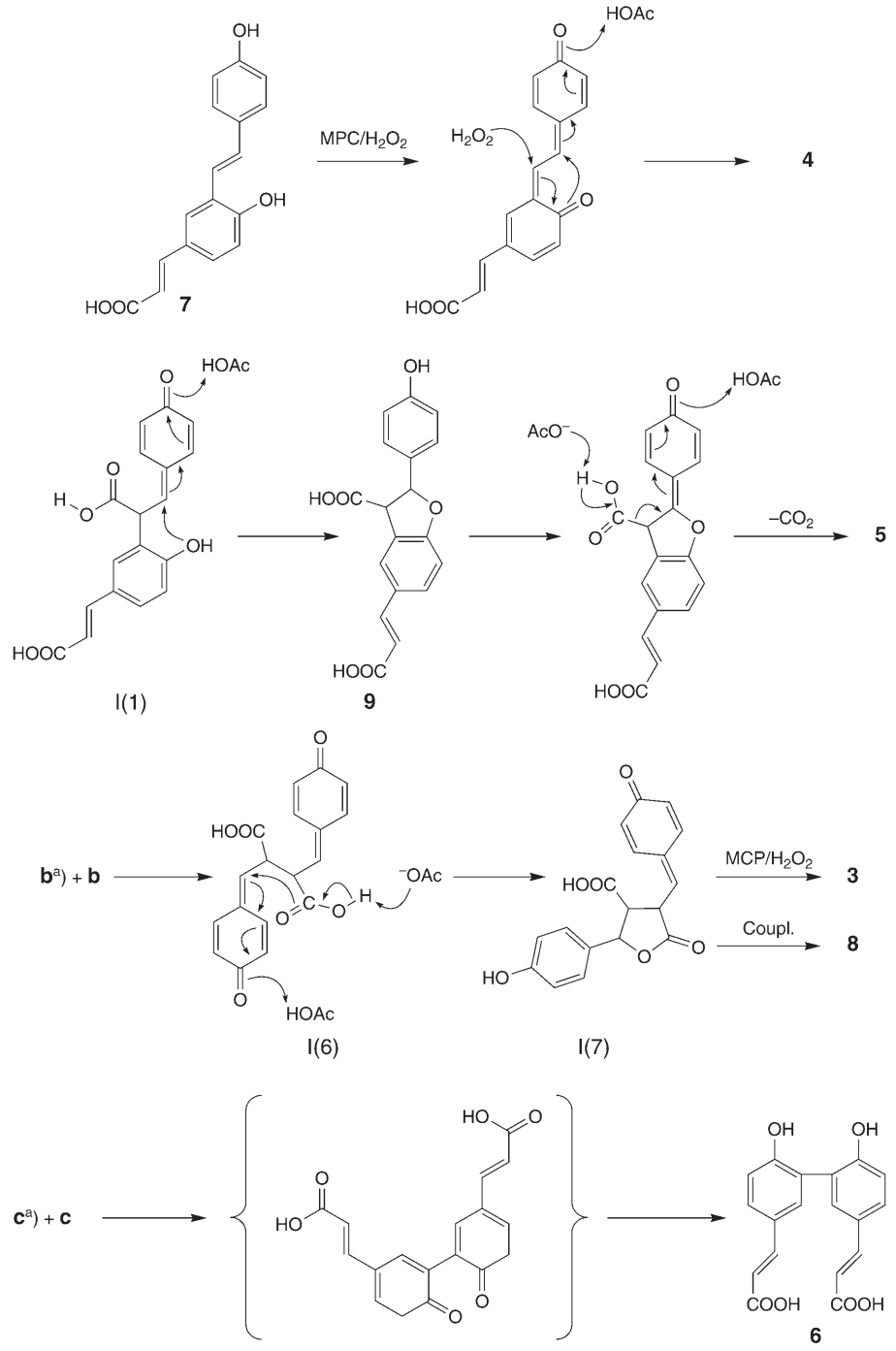

[a]) For **b** and **c**, see *Scheme 1* or *2*.

Testing of the antioxidant activity of triCA3 (*cis*-**2**), diCA1 (**3**), diCA5 (**7**), and diCA7 (**9**) revealed that they are stronger antioxidants than the parent compound CA. Their antioxidant activity appears to be related to the existence of a fully conjugated structure in the molecule. Research is currently being undertaken to identify microcrystalline components appearing in the 19 peaks shown in the LC/MS^3 measurement (*Fig. 2*).

This investigation was supported by the *Specialized Research Fund for the Doctoral Program of Higher Education* (No. 20040316002), P. R. China. We thank Dr. *Bin Ma*, School of Pharmacy, Shandong University, China, for the 2D-NMR experiments.

REFERENCES

[1] L. Ou, L. Y. Kong, X. M. Zhang, M. Niwa, *Biol. Pharm. Bull.* **2003**, *26*, 1511.
[2] H. L. Liu, L. Y. Kong, Y. Takaya, M. Niwa, *Chem. Pharm. Bull.* **2005**, *53*, 816.
[3] H. Kikuzaki, M. Hisamoto, K. Hirose, K. Akiyama, H. Taniguchi, *J. Agric. Food Chem.* **2002**, *50*, 2161.
[4] R. B. Cain, R. F. Bilton, J. A. Darrah, *Biochem. J.* **1968**, *108*, 797.
[5] D. Parke, F. Rynne, A. Glenn, *J. Bacteriol.* **1991**, *173*, 5546.
[6] D. Delneri, G. Degrassi, R. Rizzo, C. V. Bruschi, *Biochem. Biophys. Acta* **1995**, *1244*, 363.
[7] P. Gramatica, B. M. Ranzi, P. Manitto, *Bioorg. Chem.* **1981**, *10*, 14.
[8] P. Chatonnet, Boidron J. N. Dubourdieu, M. Pons, *J. Sci. Food Agric.* **1992**, *60*, 165.
[9] J. Cavin, J. F. Cavin, V. Dartois, C. Divies, *Appl. Environ. Microbiol.* **1998**, *64*, 1466.
[10] Y. Suezawa, N. Yoshioka, H. Mori, *Nippon Nogei Kagaku Kaishi* **1998**, *72*, 43.
[11] L. Barthelmebs, C. Divies, J. F. Cavin, *Appl. Environ. Microbiol.* **2000**, *66*, 3368.
[12] A. M. D. Nambudiri, J. V. Bhat, P. V. Subba Rao, *Biochem. J.* **1972**, *130*, 425.
[13] A. M. D. Nambudiri, C. P. Vance, G. H. N. Towers, *Biochim. Biophys. Acta* **1974**, *343*, 148.
[14] G. Degrassi, P. P. De Laureto, C. V. Bruschi, *Appl. Environ. Microbiol.* **1995**, *61*, 326.
[15] D. A. N. Edlin, A. Narbad, M. J. Gasson, J. R. Dickinson, D. Lloyd, *Enzyme Microb. Technol.* **1998**, *22*, 232.
[16] J. L. Torres y Torres, J. P. N. Rosazza, *J. Nat. Prod.* **2001**, *64*, 1408.
[17] N. Habu, M. Samejima, T. Yoshimoto, G. Mokuzai, *Mokuzai Gakkaishi* **1988**, *34*, 1026.
[18] J. M. Marita, W. Vermerris. J. Ralph, R. D. Hatfield, *J. Agric. Food Chem.* **2003**, *51*, 1313.
[19] M. Antolovich, D. R. J. Bedgood, A. G. Bisshop, D. Jardine, P. D. Prenzler, K. Robards, *J. Agric. Food Chem.* **2004**, *52*, 962.
[20] H. Z. Pan, L. M. Feng, H. Lu, C. M. Xu, P. C. Zhang, Z. N. Zhang, *Chin. Med. Sci. J.* **1998**, *13*, 20.

Received January 15, 2007